



Cite this: *Phys. Chem. Chem. Phys.*,
2017, **19**, 4734

Trapping of excess energy in a nano-layered microenvironment to promote chemical reactions

V. Ramakrishnan,^a Y. Nabetani,^{†*ab} D. Yamamoto,^{ab} T. Shimada,^{ab} H. Tachibana^{ab}
and H. Inoue^{*ab}

Nano-layered hybrid compounds composed of a polyfluoroalkyl azobenzene surfactant (abbreviated as C3F-Azo-C6H) and layered inorganic nanosheets undergo three-dimensional morphological changes such as reversible shrinkage and expansion of interlayer spaces, and nanosheet sliding by photo-irradiation. Previously, we have investigated the photoreactivity of C3F-Azo-C6H/clay nano-layered hybrids in various microenvironments and found a remarkable enhancement in the photoreactivity for the *cis*–*trans* photo-isomerization reaction ($\Phi_{cis-trans} = 1.9$). In this paper, nanosecond and microsecond dynamics of *trans*-C3F-Azo-C6H and its assembly in various microenvironments have been studied by laser flash photolysis to get deeper insight into the extraordinary reactivity of the molecular assembly in the nano-layered microenvironment. In solution, the molecular *trans*-C3F-Azo-C6H exhibited only a depletion of the *trans*-form of azobenzene upon the laser pulse excitation. On the other hand, in the case of the C3F-Azo-C6H/clay hybrid film, the depletion of the *trans*-form was drastically recovered in three steps on nano- and microsecond timescales. This indicates that the once reacted C3F-Azo-C6H molecule (*cis*-C3F-Azo-C6H) was reverted back to the *trans*-form after the laser pulse. It is considered that the excess energy provided by the photo-excitation, which is immediately dissipated to the surrounding media through the intermolecular vibrational modes in solution, is trapped in the nano-layered microenvironment to thermally revert the *cis*-form back to the *trans*-form. Conversely, in the case of *cis*–*trans* isomerization of the C3F-Azo-C6H/clay hybrid film upon photo-irradiation, the reactivity would be much enhanced by the additional contribution of the thermal excess energy efficiently trapped in the nano-layered microenvironment. As compared with the hydrocarbon analogue (C3H-Azo-C6H), the subsequent recovery was very much enhanced in the C3F-Azo-C6H/clay film. The polyfluoroalkyl part of the surfactant layer plays a key role in the retarded dissipation of the excess energy by photo-excitation, which might be coupled with the three-dimensional morphological motion with efficient isomerization reactions.

Received 9th December 2016,
Accepted 12th January 2017

DOI: 10.1039/c6cp08414a

rsc.li/pccp

Introduction

In the past several decades, many kinds of supra-molecular systems have been extensively studied for developing various functions such as charge separation, energy transfer, catalysis, water oxidation, and so on.^{1–4} Recently, supra-molecular systems coupled with the surrounding microenvironments have attracted much attention because of their ability to exhibit sophisticated functions.^{5–9} Among them, a layered compound is the most

interesting material which provides a microenvironment with unique characteristics such as (1) flat and smooth surfaces at the atomic level, (2) surface positive/negative charges, (3) two dimensional interlayer spaces having certain flexibility to the normal direction of the layered nanosheets, and (4) intercalation of various functional molecules.^{5,10–15}

Previously, we have reported that the interlayer distances of hybrids composed of layered compounds and cationic poly-fluorinated surfactants including an azobenzene moiety (C3F-Azo-C6H: Fig. 1a), which were originally synthesized by our group, could be successfully controlled by the mutual *trans*–*cis* isomerization upon photo-irradiation.^{7–9,16,17} Furthermore, we have found that the three-dimensional morphological change of the layered hybrid on a giant scale based on nanosheet sliding is reversibly induced by the photo-isomerization reaction of the azobenzene moiety.^{7–9} Such molecular bilayer systems coupled with layered nanosheets can be expected as a kind of artificial

^a Department of Applied Chemistry, Graduate School of Urban Environmental Sciences, Tokyo Metropolitan University, 1-1, Minami-osawa, Hachioji, Tokyo 192-0397, Japan. E-mail: yu.nabetani@cc.miyazaki-u.ac.jp, inoue-haruo@tmu.ac.jp

^b Center for Artificial Photosynthesis, Tokyo Metropolitan University, 1-1, Minami-osawa, Hachioji, Tokyo 192-0397, Japan

[†] Present address: Department of Applied Chemistry, Faculty of Engineering, University of Miyazaki, 1-1, Gakuen-kibanadai-nishi, Miyazaki-shi, Miyazaki 889-2192, Japan.

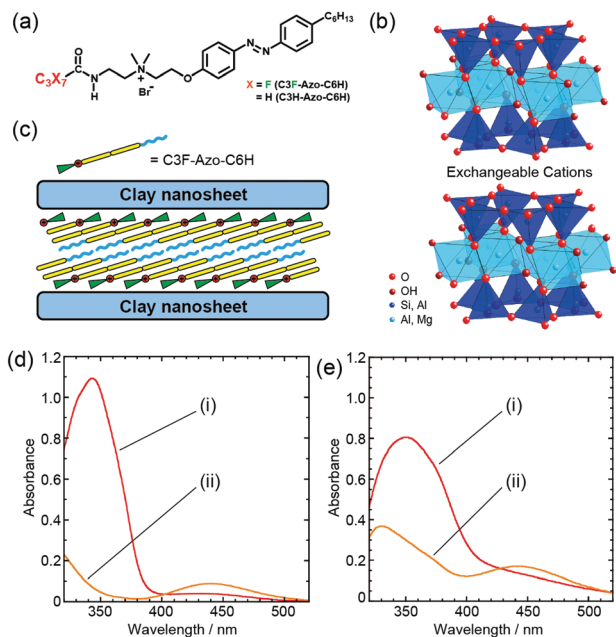


Fig. 1 Polyfluorinated surfactant including the azobenzene moiety and the clay nanosheet: (a) chemical structures of the polyfluorinated surfactant including the azobenzene moiety, (b) crystal structure of the clay nanosheet, (c) the bilayer structure of C3F-Azo-C6H/SSA, and absorption spectra of (i) *trans*- and (ii) *cis*-forms of (d) C3F-Azo-C6H in ethanol and (e) C3F-Azo-C6H/SSA films in a dry air atmosphere, respectively.

muscle model unit because the nanosheet sliding has much similarity to the contraction of animal muscles, though the sliding mechanism might be completely different from that in the muscle contraction. To apply such photo-mechanical functions and construct photo-activated devices like photo-actuators and artificial muscles, it would be essential to get deeper insight into the photoreactivity and the reaction mechanism for understanding the photo-induced morphological change of nanosheet sliding.

The photo-isomerization reactions of azobenzene and its derivatives have been actively studied by UV-vis absorption, Raman scattering, and time-resolved spectroscopy and so on for several decades.^{18–21} According to the reports, following $S_0 \rightarrow S_2$ excitation of *trans*-azobenzene in solution, the excited state is relaxed to the S_1 with a quantum yield of ~ 1 and then isomerized to the *cis*-form through the inversion mechanism.^{18,19} Such isomerization reaction processes are completed within a few ten picoseconds.^{20,21} Recently, we have systematically studied the relationship between the nanostructures of the layered clay hybrid compound intercalated with C3F-Azo-C6H (C3F-Azo-C6H/clay) and their photoreactivity for understanding the mechanism of the photo-induced morphological change and found a remarkable enhancement of photoreactivity in the nano-layered clay microenvironment.²² In particular, the *cis* to *trans* isomerization has been greatly enhanced and its quantum yield exceeds unity ($\Phi_{cis \rightarrow trans} = 1.9$), while the *trans* to *cis* isomerization is retarded conversely. Though the preference of the *trans*-form could be due to a destabilization of the *cis*-form in a rather rigid microenvironment of the interlayer space, the high quantum

yield exceeding unity required an additional rationale and factors to be operating in the interlayer space. One of the most probable phenomena could be a local heating around the molecules caused by the retarded dissipation of the excess energy provided by the photo-excitation.¹⁸ In solution the excess energy is immediately dissipated to the surrounding media through the vibrational modes within several picoseconds.^{23,24} In the interlayer space of the nano-layered hybrid, however, the dissipation of the excess energy might differ from that in solution, which leads to a local heating to enhance a thermal process reverting from the *cis*-form into the *trans*-form.

In this paper, nanosecond and microsecond dynamics of *trans*-C3F-Azo-C6H and its assembly in various micro-environments by the $\pi\text{-}\pi^*$ (S_2) excitation have been studied by means of laser flash photolysis for understanding the extraordinary photoreactivity of the molecular assembly in the nano-layered microenvironment. The recovery of the *trans*-form depletion after the photo-excitation has been successfully found in the *trans*-*cis* isomerization reaction of the C3F-Azo-C6H/clay hybrid film. The enhancement of the photoreactivity was discussed in terms of the step-wise thermal equilibration of the excess energy provided by photo-excitation in the nano-layered microenvironment.

Results and discussion

Nanosecond and microsecond dynamics of the polyfluoroalkyl azobenzene derivative, C3F-Azo-C6H, the chemical structure of which is shown in Fig. 1a, in different microenvironments were investigated by laser flash photolysis. Fig. 1d and e show the steady state absorption spectra of the *trans*- and *cis*-form of C3F-Azo-C6H in ethanol and C3F-Azo-C6H/SSA (SSA: the clay nanosheets, Smecton SA) films in a dry air atmosphere. The peaks at 344 nm and 440 nm in Fig. 1d, and 350 nm and 441 nm in Fig. 1e, which correspond to the *trans*- and *cis*-form of the azobenzene, are assigned to the $\pi\text{-}\pi^*$ and $n\text{-}\pi^*$ transitions, respectively.^{25,26} Fig. 2a shows the transient absorption spectra of *trans*-C3F-Azo-C6H in ethanol after the excitation with an excimer laser pulse ($\lambda_{\text{ex}} = 308$ nm). Just after the laser excitation ($t = 0$ μs), the transient absorption with a negative peak around 344 nm and very small positive absorption around 440 nm,

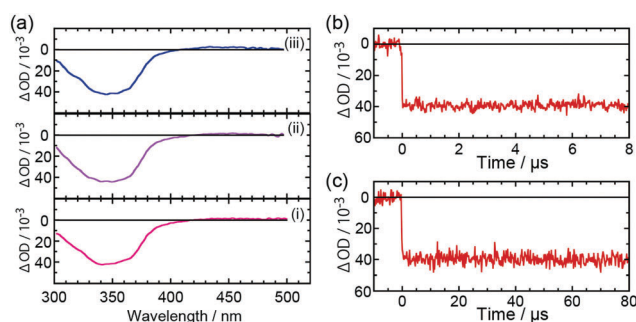


Fig. 2 (a) Transient absorption spectra of *trans*-C3F-Azo-C6H in ethanol by the excitation of 308 nm of single laser pulse (i: 0 μs , ii: 1 μs , and iii: 1 ms), and the decay observed at 365 nm in the time window of (b) 9 μs and (c) 90 μs , respectively.

which are in good agreement with the steady state absorption spectra of the *trans*- and *cis*-form of C3F-Azo-C6H in ethanol, were observed as shown in Fig. 2a(i). After 1 μ s and 1 ms, they remained unchanged as shown in Fig. 2a(ii) and (iii). The decay profile of the transient absorption observed at 365 nm also shows a sudden depletion at 0 μ s and the depletion of *trans*-C3F-Azo-C6H remains unchanged (Fig. 2b and c).

These clearly indicate the depletion of *trans*-C3F-Azo-C6H and the formation of the *cis*-form by the photo-isomerization reaction of C3F-Azo-C6H upon laser excitation. As reported earlier, photo-isomerization of azobenzene is completed within a few tens of picoseconds in solution,^{20,21} that is, the *trans*-*cis* photo-isomerization reaction of C3F-Azo-C6H in ethanol should proceed within the excitation laser pulse ($\Delta t = 12$ ns).

On the basis of the transient study in ethanol, we moved over the photochemistry of *trans*-C3F-Azo-C6H in the nano-layered microenvironment. A film sample of the hybrid compound composed of C3F-Azo-C6H and inorganic clay nanosheets (Smecton SA: SSA) was prepared. The crystal structure of the clay is shown in Fig. 1b. The intercalation of C3F-Azo-C6H into the interlayer spaces of SSA has been successfully performed by following the procedure described in the Experimental section. The detailed characterization and the nanostructure of the layered hybrid film were described in our previous report.²² C3F-Azo-C6H forms a bilayer structure within the interlayer⁸ (Fig. 1c). Fig. 3 shows the transient absorption spectra of the *trans*-C3F-Azo-C6H/SSA hybrid film in a dry air atmosphere by the excitation with an excimer laser pulse. As seen in Fig. 3a(i), the immediate depletion of *trans*-C3F-Azo-C6H was observed just after the laser excitation. Interestingly, the spectral shape of the transient absorption was delicately different from that in ethanol. The λ_{max} value of the depletion was around 370 nm at $t = 0$ μ s and gradually shifted to 380 nm with the gradual recovery of the depletion at

$t = 20$ μ s (Fig. 3a(i)-(v)). Since the starting *trans*-form in the nano-layered microenvironment has its λ_{max} at around 350 nm, the different λ_{max} (370 nm) of the depletion indicates the appearance of some other species having positive transient absorption broadened in the shorter wavelength region than the ordinary *cis*-form of azobenzene. In addition to the transient spectral characteristics, the decay profile of the depletion at 365 nm showed very different behavior from that in ethanol. After the immediate depletion at $t = 0$ μ s, a fast recovery within 1 μ s, subsequent moderate recovery within several μ s, and further slow recovery within 20 μ s were evidently observed (Fig. 3b and c). After 20 μ s of delay, both the transient absorption spectra and the time profile remained unchanged, indicating C3F-Azo-C6H in the nano-layered microenvironment reaching the final state of *trans*-*cis* isomerization of azobenzene. In general, after the photo-excitation of a molecule, the excess energy in the form of vibrational energy is immediately dissipated to the surrounding media such as solvent. The timescale of the dissipation is within ten picoseconds.^{23,24} Actually, in the femtosecond and picosecond region, it has been reported that the broadened transient spectra, which are assigned to the vibrationally hot molecule, are observed just after photo-excitation.²⁷⁻²⁹ Taking these general phenomena into consideration, the appearance of other species having positive transient absorption broadened in the shorter wavelength region than the ordinary *cis*-form of azobenzene in the transient absorption spectra described above could be closely correlated with the vibrationally excited hot molecules generated by the photo-excitation, since the hybrid film exhibits reversible interconversion repeatedly between *trans*- and *cis*-forms of azobenzene having the isosbestic point in the visible absorption spectra without forming any byproducts other than the isomers. The timescale of the relaxation, however, is very much slower than in solution. This might be characteristic in the nano-layered microenvironment.

As described in the Introduction, the extraordinary enhancement of the *cis*-*trans* isomerization of a C3F-Azo-C6H/SSA hybrid film in a dry air atmosphere and the converse retardation of the *trans*-*cis* isomerization were discussed in terms of both the destabilization of the bulky *cis*-form in a rigid microenvironment and the efficient trapping of excess energy provided by photo-excitation in the nano-layered micro-environment.²² As shown in Fig. 3b and c, the recovery rise in the time profile of the depletion of the *trans*-form observed at 365 nm indicates that *cis*-C3F-Azo-C6H once formed by the selective excitation of the *trans*-form is partly reverted back to the original *trans*-form within 20 μ s. Judging from the initial depleted absorbance ($\Delta\text{OD} = 0.05$ Fig. 3b) and the remaining one ($\Delta\text{OD} = 0.01$ Fig. 3b) after 20 μ s, the reversion reached up to nearly 80% of the once generated *cis*-form in the case. This dynamic phenomenon could be understood as a local heating around the molecule caused by the retarded dissipation of the excess energy in the nano-layered microenvironment. The local heating would preferentially populate the *trans*-form by a thermal process. Most probably, the layered nanostructure, in which C3F-Azo-C6H molecules are beautifully aligned by the introduction of a polyfluorocarbon chain (Fig. 1c), plays a key role in the retarded dissipation of the excess energy.

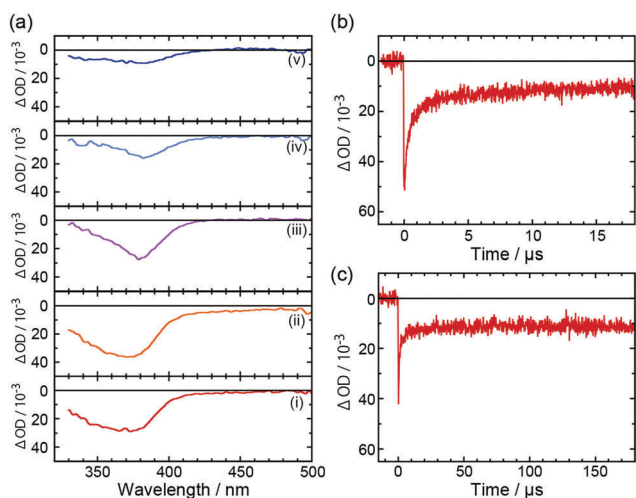


Fig. 3 Nanosecond and microsecond dynamics of the *trans*-C3F-Azo-C6H/SSA hybrid film in air by the excitation of 308 nm of single laser pulse: (a) transient absorption spectra of the hybrid film at (i) 0 μ s, (ii) 0.05 μ s, (iii) 0.15 μ s, (iv) 1.5 μ s and (v) 20 μ s, and the time profile of the depletion of the transient absorption observed at 365 nm in the time window of (b) 20 μ s and (c) 200 μ s, respectively.

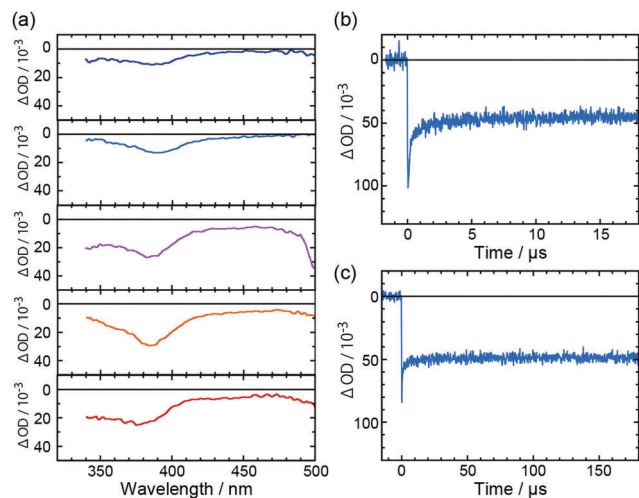


Fig. 4 Nanosecond and microsecond dynamics of a *trans*-C3H-Azo-C6H/SSA hybrid film in air by the excitation of 308 nm of single laser pulse: (a) transient absorption spectra of the hybrid film at (i) 0 μs , (ii) 0.05 μs , (iii) 0.15 μs , (vi) 1.5 μs and (v) 20 μs , and the time profiles of the depletion of the transient absorption observed at 365 nm in the time window of (b) 20 μs and (c) 200 μs , respectively.

To understand the effect of the polyfluorocarbon chain in the phenomena, the corresponding hydrocarbon analogue, C3H-Azo-C6H, in the nano-layered microenvironment was further measured by laser flash photolysis. Fig. 4a shows the transient absorption spectra of the *trans*-C3H-Azo-C6H/SSA hybrid film in a dry air atmosphere by the excitation with an excimer laser pulse. The transient spectra with a negative peak at around 375 nm at $t = 0 \mu\text{s}$, which correspond to the depletion of *trans*-C3H-Azo-C6H, were similarly observed, though the spectral shape was a little obscure. The spectral shape rapidly changed within 0.05 μs delay; the λ_{max} of the depletion rapidly red-shifted to 385 nm. Fig. 4b and c show the time profile of the transient depletion observed at 365 nm in the time window of 20 μs and 200 μs , respectively. After the photo-excitation, the initial depletion of absorption at $t = 0 \mu\text{s}$ exhibited a rapid recovery rise within 0.1 μs well in accord with the spectral change. The dynamic phenomenon looks similar to the case of the C3F-Azo-C6H/SSA film, but a bit different on the timescale and the degree of recovery from those of the polyfluorinated C3F-Azo-C6H/SSA film. The dynamic recovery rise completed within a much shorter timescale of several μs compared with $\sim 20 \mu\text{s}$ for C3F-Azo-C6H/SSA and the total reversion from the initially formed *cis*- into *trans*-form was only 50%, which is smaller than 80% for C3F-Azo-C6H/SSA (Fig. 4b). Obviously the polyfluoroalkyl chain retards the dynamics of the phenomena. Since the polyfluorocarbon chain has a smaller intermolecular interaction,^{30–32} the dissipation of the excess energy provided by photo-excitation would be certainly retarded through the polyfluoroalkylated layer in the aligned structure of the nano-layered microenvironment.

To compare the dynamic characteristics between C3F-Azo-C6H/SSA and C3H-Azo-C6H/SSA, the normalized time profiles of the signals are shown on the timescale down to nanoseconds in Fig. 5. Upon the laser flash, the initial recovery rises of the

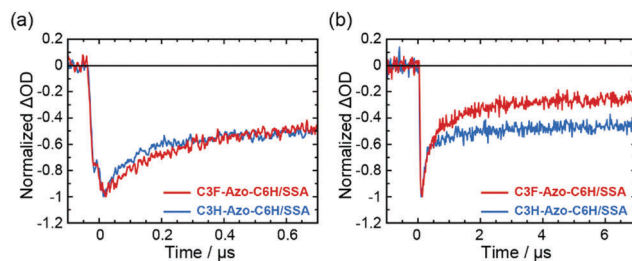


Fig. 5 Comparison of the recovery rises between C3F-Azo-C6H/SSA and C3H-Azo-C6H/SSA after the photo-excitation in the time windows of (a) 0.8 μs and (b) 8 μs .

trans-form depletion were slower in C3F-Azo-C6H/SSA than in the C3H-Azo-C6H/SSA. To get deeper insight into the dynamics, the rise components in the recovery dynamics for each hybrid film sample were analyzed by a curve fitting with exponential functions to deduce the time constants. The decay curves of the C3F-Azo-C6H/SSA film in a dry air atmosphere could be well analyzed by a sum of three exponential components with lifetimes of 0.13 μs , 1.4 μs and 8 μs along with their relative contribution (%) to the recovery of depletion (Table 1). This indicates that the reversion process from the *cis*-form back to the *trans*-form is composed of three steps, which might correspond to the dissipative relaxation of local heating through the equilibration around the neighboring molecules, and the surfactant layer within the clay nanosheet, respectively.

On the other hand, the recovery rise curve of the C3H-Azo-C6H/SSA film was well fitted by a sum of two exponential components with lifetimes of 0.1 μs and 1.3 μs as tabulated in Table 1. This indicates that the excess energy by photo-excitation in C3H-Azo-C6H/SSA is also relaxed in a step-wise manner through the equilibration with the surrounding microenvironment as well as C3F-Azo-C6H/SSA. However, the third component with the longer lifetime was not observed in the case of C3H-Azo-C6H/SSA. Moreover, the first and second rise component in the C3H-Azo-C6H/SSA became a bit faster than that in C3F-Azo-C6H/SSA. The relative contribution of each component shows different aspects between C3F-Azo-C6H/SSA and C3H-Azo-C6H/SSA. The recovery of depletion is mostly caused by the second and third component (τ_2 (49%) and τ_3 (18%)) in the C3F-Azo-C6H/SSA film, while the first component (τ_1 (70%)) has a major contribution in the C3H-Azo-C6H/SSA film. It should be noted here that C3H-Azo-C6H/SSA lacks the third component (τ_3).

Furthermore, nanosecond and microsecond dynamics of the *trans*-C3F-Azo-C6H/SSA film swelled with organic solvents observed at 365 nm were also investigated by laser flash photolysis.

Table 1 Summary of the lifetime in the decay analysis

Sample	$\tau_1/\mu\text{s}$	$\tau_2/\mu\text{s}$	$\tau_3/\mu\text{s}$
C3F-Azo-C6H/SSA film in dry air	0.13 (33%)	1.4 (49%)	8 (18%)
C3H-Azo-C6H/SSA film in dry air	0.10 (70%)	1.3 (30%)	—
C3F-Azo-C6H/SSA moisturized with <i>n</i> -hexane	0.18 (35%)	2.3 (10%)	12 (55%)

Relative contribution to the recovery of depletion is indicated in the parentheses (%).

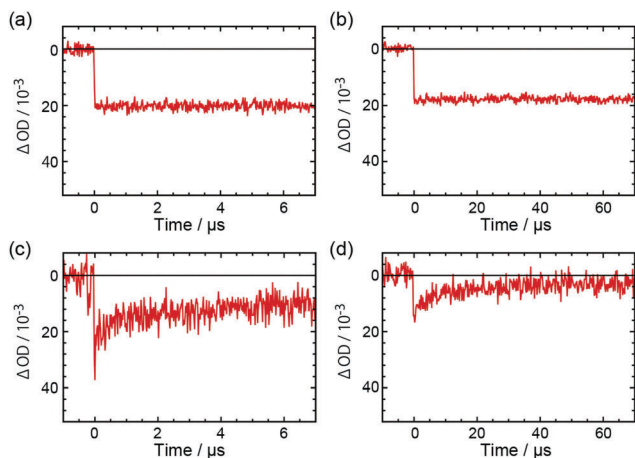


Fig. 6 Rise and decay curves of C3F-Azo-C6H/SSA in (a and b) benzene and (c and d) *n*-hexane, respectively.

In the previous study of the C3F-Azo-C6H/SSA in various micro-environments, it was revealed that the photoreactivity of the C3F-Azo-C6H/SSA film was drastically changed by moisturizing with organic solvents; the hybrid film swelled with benzene had a much smaller quantum yield than the dried film, while the hybrid film moisturized with *n*-hexane maintains the high quantum yield.²² It should be thus curious to compare the dynamics of the transient depletion between the two conditions and how they are different from that of the dried film. Fig. 6 shows the decay curve of transient absorption of the C3F-Azo-C6H/SSA film being swelled with benzene and *n*-hexane by the excitation of an excimer laser pulse. In the case of the C3F-Azo-C6H/SSA film swelled with benzene, a sudden depletion of the transient absorption was observed without exhibiting any recovery phenomena to remain unchanged, as shown in Fig. 6a and b. This is very similar to the case of C3F-Azo-C6H in ethanol. When swelled with benzene, the interlayer clearance space of the hybrid, C3F-Azo-C6H/SSA, expands up to 3.62 nm from the dried one (3.39 nm), and benzene molecules penetrate into the interlayer to surround the azobenzene moiety. The excess energy by the photo-excitation could be thus immediately dissipated to the surrounding benzene molecules. The fast cooling down through the surrounding benzene molecules would efficiently prevent the reversion back to the *trans*-form by the thermal process.

On the other hand, in the case of the C3F-Azo-C6H/SSA film moisturized with *n*-hexane, the depletion of the *trans*-form was again recovered in a step-wise fashion after the photo-excitation similar to the hybrid film in a dry air atmosphere, though the signal to noise ratio in the decay curve is rather low (Fig. 6c and d). Since the interlayer clearance space of the hybrid, C3F-Azo-C6H/SSA, remains unchanged (3.39 nm) even upon prolonged moisturizing with *n*-hexane, which is not able to penetrate into the interlayer spaces of the C3F-Azo-C6H/SSA as reported previously, it does not act as a heat conductor.²² The recovery rise curve for C3F-Azo-C6H/SSA moisturized with *n*-hexane was also analyzed by a sum of three exponential components the time constants of which are similar to those

of the C3F-Azo-C6H/SSA film in a dry air atmosphere as summarized in Table 1, though the accuracy of analysis is not so good due to the low signal to noise ratio.

The striking difference of the transient behaviour strongly supports the postulate that the recovery rise phenomena observed in the transient depletion in the cases of the hybrid film in a dry air atmosphere and moisturized with *n*-hexane surely express a thermal process induced by a local heating by a retarded dissipation of excess energy upon light absorption, when compared with the normal sudden depletion to remain unchanged without any recovery in solution and in the hybrid swelled with benzene. The excess energy in the vibrationally hot state of the molecule in solution is efficiently dissipated through the surrounding solvent molecules which are mobile and readily dissipate the excess energy through intermolecular V-V and V-T relaxation to have a short lifetime within several picoseconds, while the beautifully aligned and rigidly packed bilayer structure in the nano-layered hybrid having very limited mobility of each surfactant chains would not suffer effective intermolecular V-V and V-T relaxation processes to allow a rather long lifetime of the hot states. The heat dissipation mechanism in the C3F-Azo-C6H/SSA film by photo-excitation is thus summarized as a schematic illustration in Fig. 7. The excess energy provided by the photo-excitation is gradually dissipated in the nano-layered microenvironment. The step-wise thermal equilibration of the excess energy might be explained as follows. Firstly, the excess energy is equilibrated within the neighboring molecules of the azobenzene moiety ($\tau_1 = 0.13 \mu\text{s}$) after the Frank-Condon relaxation within a molecule and the *trans-cis* isomerization reaction. Subsequently, it is equilibrated within the hydrocarbon chains of the surfactant layer ($\tau_2 = 1.4 \mu\text{s}$), and finally done within the whole bilayer surfactant molecules including the polyfluoroalkyl parts in the clay nanosheets ($\tau_3 = 8 \mu\text{s}$). The lack of the third component (τ_3) in C3H-Azo-C6H/SSA (Table 1) strongly suggests that the polyfluoroalkylated layer in the hybrid film, C3F-Azo-C6H/SSA, causes the slowest heat dissipation due to the weak intermolecular interaction to lengthen the “local-heating,” while the heat dissipation is completed in the second component (τ_2) among the whole hydrocarbon chains in the case of

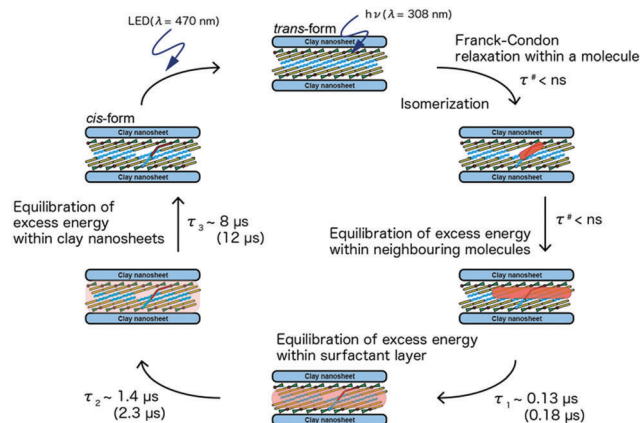


Fig. 7 A schematic illustration of the step-wise equilibration of excess energy in the nano-layered microenvironment.

C3H-Azo-C6H/SSA. It can be considered that the excess energy efficiently trapped in the nano-layered microenvironment wholly retards the *trans*-*cis* isomerization by thermally inducing the *cis*-*trans* back isomerization. Conversely, in the *cis*-*trans* isomerization, the whole reactivity would be enhanced by the further addition of the thermal contribution. Therefore, the high quantum yield exceeding unity ($\Phi = 1.9$) is achieved in the *cis*-*trans* isomerization reaction. On the other hand, the excess energy is provided by the photo-excitation in the case of C3H-Azo-C6H, and the subsequent dissipation of the excess energy is completed within the second step (τ_2) with limited reversion from the once generated *cis*-form back to the *trans*-form, which leads to the smaller quantum yield ($\Phi = 0.42$) for *cis*-*trans* isomerization.²² The interesting extraordinary enhancement and retardation of the *trans*-*cis* isomerization in the nano-layered micro-environment are thus rationalized by the mechanism. The nanostructure of the layered hybrids and the well aligned bilayer polyfluorinated surfactant play a synergetic role in the efficient trapping of the excess energy. The heat trapping might cause one of the key factors in the three-dimensional morphological changes like a sliding of nanosheets.⁷⁻⁹

Experimental

Materials

A cationic polyfluorinated azobenzene surfactant (C3F-Azo-C6H) and its hydrocarbon analogue (C3H-Azo-C6H) were synthesized by following the procedure reported previously.^{30,31} Ethanol (Spectroscopic grade, Kanto Chemical), benzene (Spectroscopic grade, Kanto Chemical) and *n*-hexane (Spectroscopic grade, Kanto Chemical) were purchased and used without further purification. The synthetic inorganic nanosheet, Sumecton SA (SSA), the chemical structure of which is shown in Fig. 1c, was provided by Kunimine Industries and used without further purifications. An ion-exchanged water ($< 0.1 \mu\text{S cm}^{-1}$) was used for the synthesis of the layered hybrids.

Sample preparation, characterization, and photoreaction

SSA (300 mg) was dispersed in 300 mL of ion-exchanged water and used as a stock dispersion for the hybrid preparation. An aliquot of C3F-Azo-C6H aqueous solution in 15 eq. of loading level *versus* the cation exchange capacity (CEC) of SSA was added to 10 mL of the SSA aqueous dispersion and stirred at 70 °C for 5 hours to precipitate the hybrid compound. The mixture was filtered by a hydrophilic polytetrafluoroethylene (PTFE) membrane (Pore diameter: 0.1 μm , Advantec) and washed with the ion-exchanged water. After the filtration, the C3F-Azo-C6H/SSA hybrids collected were dried in a vacuum and stored in the dark. The dried hybrid samples were characterized by thermogravimetric/differential analysis, X-ray diffraction measurements and UV-visible absorption spectroscopy as described in our previous report.²² To prepare the hybrid films, an appropriate amount of C3F-Azo-C6H/SSA hybrid dispersed in *n*-hexane was cast over a cleaned cover glass. Before the experiments, the sample films were placed in the incubator at 50 °C for 3 hours to ensure that the C3F-Azo-C6H

was all converted to the *trans*-form in the dark. In the photo-reaction, 365 nm and 470 nm of light emitting diodes (LEDs) were used as excitation light sources for the *trans*- and *cis*-form of the azobenzene surfactants.

Laser flash photolysis

Laser flash photolysis was performed using a XeCl excimer laser (LUMONICS Hyper EX-300, 308 nm, $\Delta t = 12$ ns fwhm) for photo-excitation and a LED (ZUV-H20MC, 365 nm, OMRON) used as a monitoring light source equipped with a detection system composed of a monochromator (MC-30, 1200G/mm, RITSU OYO KOGAKU) and a photomultiplier tube (R-636, HAMAMATSU PHOTONICS). The amplified signal was recorded on a digital storage oscilloscope (TDS620A, Tektronix). Transient absorption spectra were obtained using a spectrometric multichannel analyzer (SMA: IRY-512, Princeton Instruments) equipped with a polychromator (Monospec-27, Jarrell-Ash). The pulsed xenon flash lamp (Tokyo Instruments XF-80) was used as a probe light for the spectral measurement and the timing to the excitation pulse was controlled by a digital delay/pulse generator (DG535, Stanford Research Systems). The film sample was irradiated with the excitation pulse (0.45 mJ per mm per pulse) at an angle of 45° against the probe light. The spectra and time profiles of decay curves were obtained by averaging 120 spectra and 360 curves of the sample excited with a single shot pulse, respectively. The samples were replaced with the fresh ones or *trans*-rich-ones ensured by the irradiation with a LED light (470 nm, Mightex Systems) for 30 seconds to revert back to the *trans*-rich-form of azobenzene at each excitation. In the experiment for a solvent-moisturized hybrid film, the sample was immersed in benzene or *n*-hexane in a quartz cell (optical length: 1 cm). All spectral measurements were carried out at room temperature (294 K).

Conclusions

In this study, nanosecond and microsecond dynamics of *trans*-C3F-Azo-C6H in nano-layered microenvironments by the π - π^* (S_2) excitation have been studied by laser flash photolysis to get deeper insight into the extraordinary reactivity of the molecular assembly in the nano-layered microenvironment. In the *trans*-*cis* isomerization of the C3F-Azo-C6H/SSA hybrid film, it has been successfully observed for the first time that the depletion of the *trans*-form is drastically recovered in a step-wise fashion. This indicates that the once photoreacted C3F-Azo-C6H molecule into the *cis*-form is again reverted back to the *trans*-form on the nano- and microsecond timescale. The excess energy provided by the photo-excitation, which is efficiently trapped as a “local-heating” in the nano-layered structure, preferentially populates the *trans*-form by a thermal process. This is the first report of demonstrating a “local-heating” in the nano-layered microenvironment. The surfactant layer, especially the polyfluoroalkylated layer, plays a key role in the retarded dissipation of the excess energy by photo-excitation, which might be coupled with the three-dimensional morphological motion triggered by efficient isomerization reactions.

Acknowledgements

This work was partially supported by a Grant-in-Aid for Young Scientists (B) from the Ministry of Education, Culture, Sports, Science and Technology of Japan.

Notes and references

- 1 J.-M. Lehn, *Supramolecular Chemistry: Concepts and Perspectives*, VCH, Weinheim, 1995.
- 2 D. R. Weinberg, C. J. Gagliardi, J. F. Hull, C. F. Murphy, C. A. Kent, B. C. Westlake, A. Paul, D. H. Ess, D. G. McCafferty and T. J. Meyer, *Chem. Rev.*, 2012, **112**, 4016–4093.
- 3 J. D. Blakemore, R. H. Crabtree and G. W. Brudvig, *Chem. Rev.*, 2015, **115**, 12974–13005.
- 4 E. E. Benson, C. P. Kubiak, A. J. Sathrum and J. M. Smieja, *Chem. Soc. Rev.*, 2009, **38**, 89–99.
- 5 Y. Ishida, T. Shimada, D. Masui, H. Tachibana, H. Inoue and S. Takagi, *J. Am. Chem. Soc.*, 2011, **133**, 14280–14286.
- 6 Y. Ishida, T. Shimada, H. Tachibana, H. Inoue and S. Takagi, *J. Phys. Chem. A*, 2012, **116**, 12065–12072.
- 7 Y. Nabetani, H. Takamura, Y. Hayasaka, T. Shimada, S. Takagi, H. Tachibana, D. Masui, Z. Tong and H. Inoue, *J. Am. Chem. Soc.*, 2011, **133**, 17130–17133.
- 8 Y. Nabetani, H. Takamura, Y. Hayasaka, S. Sasamoto, Y. Tanamura, T. Shimada, D. Masui, S. Takagi, H. Tachibana, Z. Tong and H. Inoue, *Nanoscale*, 2013, **5**, 3182–3193.
- 9 Y. Nabetani, H. Takamura, A. Uchikoshi, S. Z. Hassan, T. Shimada, S. Takagi, H. Tachibana, D. Masui, Z. Tong and H. Inoue, *Nanoscale*, 2016, **8**, 12289–12293.
- 10 K. Takagi, H. Usami, H. Fukaya and Y. Sawaki, *J. Chem. Soc., Chem. Commun.*, 1989, 1174–1175.
- 11 K. Takagi, T. Kurematsu and Y. Sawaki, *J. Chem. Soc., Perkin Trans. 2*, 1991, 1517–1522.
- 12 M. Ogawa and K. Kuroda, *Chem. Rev.*, 1995, **95**, 399–438.
- 13 T. Yui, S. R. Uppili, T. Shimada, D. A. Tryk, H. Yoshida and H. Inoue, *Langmuir*, 2002, **18**, 4232–4239.
- 14 S. Takagi, M. Eguchi, D. A. Tryk and H. Inoue, *J. Photochem. Photobiol., C*, 2006, **7**, 104–126.
- 15 M. Ogawa, K. Saito and M. Sohmiya, *Dalton Trans.*, 2014, **43**, 10340–10354.
- 16 Z. Tong, S. Takagi, T. Shimada, H. Tachibana and H. Inoue, *J. Am. Chem. Soc.*, 2006, **128**, 684–685.
- 17 Z. Tong, S. Sasamoto, T. Shimada, S. Takagi, H. Tachibana, X. Zhang, D. A. Tryk and H. Inoue, *J. Mater. Chem.*, 2008, **18**, 4641–4645.
- 18 T. Fujino, S. Y. Arzhantsev and T. Tahara, *Bull. Chem. Soc. Jpn.*, 2002, **75**, 1031–1040.
- 19 T. Fujino and T. Tahara, *J. Phys. Chem. A*, 2000, **104**, 4203–4210.
- 20 I. K. Lednev, T.-Q. Ye, R. E. Hester and J. N. Moore, *J. Phys. Chem.*, 1996, **100**, 13338–13341.
- 21 M. Terazima, M. Takezaki, S. Yamaguchi and N. Hirota, *J. Chem. Phys.*, 1998, **109**, 603–609.
- 22 V. Ramakrishnan, D. Yamamoto, S. Sasamoto, T. Shimada, Y. Nabetani, H. Tachibana and H. Inoue, *Phys. Chem. Chem. Phys.*, 2014, **16**, 23663–23670.
- 23 J. B. Birks, *Photophysics of Aromatic Molecules*, John Wiley & Sons, Ltd, New York, 1970.
- 24 V. R. N. J. Turro and J. C. Scaiano, *Principles of Molecular Photochemistry An Introduction*, University Science Book, California, 2009.
- 25 P. P. Birnbaum, J. H. Linford and D. W. G. Style, *Trans. Faraday Soc.*, 1953, **49**, 735–744.
- 26 H. M. D. Bandara and S. C. Burdette, *Chem. Soc. Rev.*, 2012, **41**, 1809–1825.
- 27 R. J. Sension, S. T. Repinec, A. Z. Szarka and R. M. Hochstrasser, *J. Chem. Phys.*, 1993, **98**, 6291–6315.
- 28 P. Hamm, S. M. Ohline and W. Zinth, *J. Chem. Phys.*, 1997, **106**, 519–529.
- 29 T. Fujino, S. Y. Arzhantsev and T. Tahara, *J. Phys. Chem. A*, 2001, **105**, 8123–8129.
- 30 Y. Kameo, S. Takahashi, M. Krieg-Kowald, T. Ohmachi, S. Takagi and H. Inoue, *J. Phys. Chem. B*, 1999, **103**, 9562–9568.
- 31 H. Kusaka, M. Uno, M. Krieg-Kowald, T. Ohmachi, S. Kidokoro, T. Yui, S. Takagi and H. Inoue, *Phys. Chem. Chem. Phys.*, 1999, **1**, 3135–3140.
- 32 T. Yui, H. Yoshida, H. Tachibana, D. A. Tryk and H. Inoue, *Langmuir*, 2002, **18**, 891–896.